

# AIRS Radiance Validation Over Ocean From Sea Surface Temperature Measurements

Denise E. Hagan<sup>a</sup> and Peter J. Minnett<sup>b</sup>

<sup>a</sup>Jet Propulsion Laboratory, California Institute of Technology  
4800 Oak Grove Drive, Pasadena, CA 91109  
818-354-7073

<sup>b</sup>Rosenstiel School of Marine and Atmospheric Sciences  
University of Miami, Miami, FL

*Abstract* --The objective of this paper is to demonstrate the accuracy of methods and in situ data for early validation of calibrated Earth scene radiances measured by the Atmospheric InfraRed Sounder (AIRS) on the *Aqua* spacecraft. We describe an approach for validation that relies on comparisons of AIRS radiances with drifting buoy measurements, ship radiometric observations and mapped sea surface temperature products during the first six months after launch. The focus of the validation is on AIRS channel radiances in narrow spectral window regions located between 800-1000  $\text{cm}^{-1}$  and between 2500 and 2700  $\text{cm}^{-1}$ . Simulated AIRS radiances adjusted to the surface are compared to SST observations co-located in time and space, to demonstrate accuracies that can be achieved in clear atmospheres. An error budget, derived from single channel, single footprint matchups, suggests AIRS can be validated to better than 1% in absolute radiance during early mission operations. The goal is to validate instrument radiances close to the demonstrated pre-launch calibration accuracy of about 0.4 % (equivalent to 0.2 K in brightness temperature, at 300 K and 938  $\text{cm}^{-1}$ ).

## TABLE OF CONTENTS

1. INTRODUCTION
2. SPECTROMETER MEASUREMENTS
3. VALIDATION DATA SOURCES
4. VALIDATION IN THE FIRST THREE MONTHS
5. VALIDATION IN THE FIRST SIX MONTHS
6. SUMMARY

1. INTRODUCTION

The Atmospheric Infrared Sounder (AIRS) will fly onboard the NASA Earth Observing Satellite (EOS) polar-orbiting *Aqua* spacecraft. The AIRS is a high-resolution infrared spectrometer designed to

provide atmospheric temperature and moisture profiles at least as accurate as those measured by standard radiosondes (Aumann et al., 2002). The spatial resolution of the instrument at nadir is approximately 15  $\text{km}^2$ . The noise equivalent temperature difference (NE $\Delta$ T) of the detectors is typically 0.1 to 0.3 K, with a required absolute measurement accuracy of 3%. At "first light" the aperture of the instrument will be opened to view Earth. During this early period of instrument operation, the accuracy of the satellite measurements will be assessed based on incomplete knowledge of instrument and data software performance. The blackbody radiance determination will rely on pre-launch measurements and models to assign spectral response functions to the detector focal plane array (Strow et al., 2002).

Several issues may contribute to ambiguities in instrument response. While the AIRS channel radiances will be calibrated to the onboard blackbody target once per cross-track scan, uncertainties in scan angle dependent view factors, the spectral response of the detection system, or incomplete knowledge of the on-board calibrators will require resolution using independent validation sources.

We have chosen an approach for early assessment of the accuracy of the measured radiance that is not dependent on an exact knowledge of the instrument spectral responses. In order to carry out initial checks of the accuracy of the radiation measurements and minimize calibration uncertainties, simple validation techniques will be implemented that operate in atmospheric "window" regions or spectral regions relatively void of gas absorption features. This work focuses on spectral regions located in the well-known atmospheric windows located between 2500-2700  $\text{cm}^{-1}$  and 800-1200  $\text{cm}^{-1}$  (3.7-4.0  $\mu\text{m}$  and 8.3-12.5  $\mu\text{m}$ ). While the latter spectral region is affected by water vapor continuum absorption and emission, it is relatively

void of strong water vapor lines and trace gas absorption features, and hence is considered a window region.

Pre-launch thermal-vacuum blackbody calibration results indicate that, using a reasonable cross-section of detectors, it should be possible to extrapolate the performance of a sparse set of detectors to the general state of the instrument calibration (Pagano et al., 2002). There are several candidate spectral regions that are "wide" enough such that small uncertainty in the assignment of spectral wavelength to detector channel does not introduce large errors in the equivalent blackbody radiance. For example, within small sub-bands in the super-transparent regions located between 2500 to 2700  $\text{cm}^{-1}$ , the radiation at the entrance aperture of AIRS should be very similar to the radiation leaving the surface.

For the AIRS detection wavelengths, the sea surface emission is near unity. Away from strong ocean current regimes, the sea surface is relatively uniform in temperature in well-mixed wind regimes. Because of these reasons, early validation techniques in the first three months of the Aqua mission will use basic statistical methods to check the radiances in AIRS window channels against sea surface temperatures (SST) derived from the daily NCEP (National Center for Environmental Prediction) real-time, global, sea surface temperature (RTG-SST) analysis and the weekly Reynolds's Sea Surface Temperature climate product (Reynolds and Smith, 1994). During this period and the following three months of observations, more accurate point comparisons will be derived from match-ups of AIRS observations with drifting buoy and ship radiometric measurements. These comparisons will be used to help assess the state of the instrument accuracy for a required re-delivery of the AIRS radiance calibration software to the GFSC DAAC seven months after launch.

We provide in the body of this paper examples of comparisons of simulated AIRS radiances with the different SST sources and the expected error budget. The goal of the validation effort is to demonstrate radiometric measurement accuracy that approaches the instrument absolute calibration accuracy of 0.2 K, as demonstrated through pre-launch calibrations (Pagano et al., 2002). The paper is arranged with descriptions of the data sources and their accuracies, followed by demonstrations of the techniques to be used for AIRS radiance

validation in the first six months of instrument operation.

## 2. SPECTROMETER MEASUREMENTS

The spectrum of Figure 1 represents AIRS equivalent brightness temperatures at the top of the atmosphere for a single nadir footprint over the tropical ocean in clear sky conditions. The

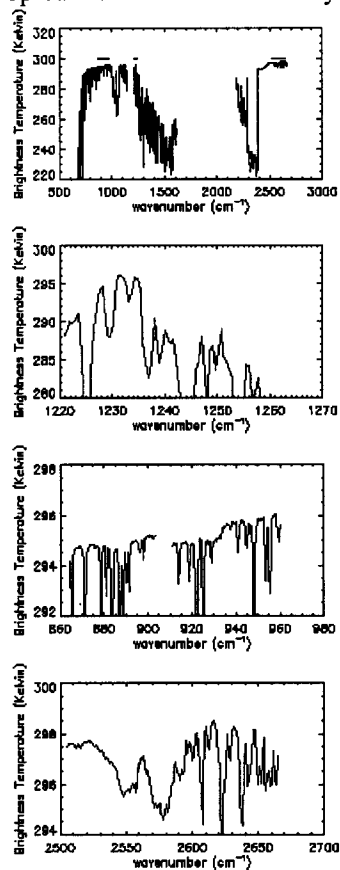


Figure 1. (a) Spectrum of simulated AIRS top-of-atmosphere equivalent brightness temperature with wavelength over the tropical ocean. Solid lines in Figure 1a designate spectral regions evaluated in this paper. These regions are shown in expanded form in (b) through (d).

spectrum was generated from line-by-line radiative transfer calculations that are convolved with the AIRS spectral response functions (Strow et al. 2002). The candidate window regions to be used for validation purposes are the commonly called "atmospheric window regions" shown by solid lines. Within these larger spectral regions are sub-regions generally two to three wavenumbers wide that are measured by four to six AIRS detectors. These regions are shown in expanded form in Figure 1b-d. The wavelengths corresponding to the

central detectors are listed in Table 1. The central and neighboring detectors are believed to lie well within the error margins of spectral uncertainty for measurements at first light (Strow et al., 2002), with the possible exceptions of the very narrow bands located at 1232 cm<sup>-1</sup> and 1235 cm<sup>-1</sup>.

The instrument noise equivalent temperature difference (NEAT) and absolute accuracy relative to a NIST traceable blackbody for the central detector

of each sub-region are provided in Table 1. The temperature uncertainty related to spectral fitting of line models to laboratory measurements is thought to be negligible in the windows relative to other error sources (Strow et al., 2002). As described by Aumann et al. (2002), the detection system is redundant, and hence for the present set of detectors, the noise can be reduced by a square root factor in a given sub-region. The effective band noise is generally half of the detector NEAT.

Table 1. Instrument measurement uncertainties (Kelvin) for central detectors of AIRS spectral window regions. Values listed only once hold for all wavelengths. A null value indicates similar uncertainty as preceding wavelength. Uncertainties related to models and SST in situ measurements are also provided.

| Spectral wave-length (cm <sup>-1</sup> ) | NEAT detector | Absolute accuracy <sup>§</sup> | Surface emissivity | RTA 10% H <sub>2</sub> O | Parameterization +1K bias | Drifting buoy accuracy <sup>†</sup> | Cloud filter bias <sup>*</sup> | Sea surface skin effect |
|--|---------------|--------------------------------|--------------------|--------------------------|---------------------------|-------------------------------------|--------------------------------|-------------------------|
| 868                                      | 0.22          | 0.25                           | 0.02               | 0.2                      | 0.40                      | 0.97                                | 0.1                            | 0.2                     |
| 885                                      | 0.20          | 0.20                           |                    |                          |                           |                                     |                                |                         |
| 893                                      | 0.19          |                                |                    |                          |                           |                                     |                                |                         |
| 900                                      | 0.17          |                                |                    |                          |                           |                                     |                                |                         |
| 938                                      | 0.14          |                                | 0.02               |                          | 0.33                      | 0.82                                | 2.4                            |                         |
| 943                                      | 0.14          |                                |                    |                          |                           |                                     |                                |                         |
| 951                                      | 0.13          |                                |                    |                          |                           |                                     |                                |                         |
| 957                                      | 0.13          |                                |                    |                          |                           |                                     |                                |                         |
| 963                                      | 0.12          |                                |                    |                          |                           |                                     |                                |                         |
| 968                                      | 0.12          |                                |                    |                          |                           |                                     |                                |                         |
| 1232                                     | 0.11          | 0.10                           |                    |                          | 0.23                      | 0.58                                |                                |                         |
| 1234                                     | 0.11          |                                |                    |                          |                           |                                     |                                |                         |
| 2522                                     | 0.31          |                                |                    |                          |                           |                                     |                                |                         |
| 2561                                     | 0.33          | 0.15                           |                    |                          |                           |                                     |                                |                         |
| 2616                                     | 0.33          | 0.20                           | 0.011              |                          | 0.02                      | 0.05                                | 1.6                            |                         |
| 2632                                     | 0.39          |                                |                    |                          |                           |                                     |                                |                         |
| 2646                                     | 0.40          |                                |                    |                          |                           |                                     |                                |                         |

<sup>§</sup> The absolute accuracy is relative to a NIST traceable blackbody target located at nadir viewing position (Pagano et al., 2002).

<sup>†</sup> This is the drifter deployment accuracy. A study by Emery et al. (2001) suggests that operational drifters located within a radius of 50 km can differ by as much as 0.4 K in the open ocean.

<sup>\*</sup> The uncertainty estimate assumes that 10% of an AIRS field-of-view is contaminated by a cloud radiating at 265 K.

### 3. VALIDATION DATA SOURCES

The primary source of real-time SST observations is the National Oceanographic and Atmospheric Administration (NOAA) NCEP. This archive is comprised of hourly to daily reports from merchant ships, drifting buoys, moored buoys and the Coastal Marine Automated Network. Using statistics based on separation distances, Emery et al. (2001) discuss the accuracy and consistency of merchant ship data relative to drifting buoy data. They find that while the geographic coverage provided by ships is excellent, biases and root-mean-square errors are

higher than those of drifting buoy data. The statistics of ship observations are 0.15 K ± 1.2 K. Their analyses suggest that due to natural variability of the local SST field, calibration and other sensor errors, drifting buoy data that fall within a radius of 50 km are self consistent to within a mean difference of 0.05 K and standard deviation of 0.4 K. They attribute the smaller variability of the drifting buoy data to better sensor calibration. Drifting buoy sensors are calibrated to 0.1°C prior to deployment, whereas merchant ship data often have no record of traceable calibration. In addition, the depth and structure of the ocean thermocline and near surface temperature gradient

contribute variability between measurements. Merchant ship observations are usually acquired in a water intake region in the hull of the ship that can occur at depths several to tens of meters below the water surface. Drifting buoy data are acquired 0.5 to 1 m below the surface depending on wave conditions. Kilpatrick et al. (2001) suggest an accuracy in their satellite-based Pathfinder SST product relative to buoy observations of  $0.1 \pm 0.5$  K, consistent with the findings of Emery et al. (2001). Merchant and Harris (1999) and Harris and Saunders (1996) have also used drifting and fixed buoy data to ascertain biases in the Along Track Scanning Radiometer (ATSR) satellite measurements. Based on historical references, buoy measurements are probably the best readily available source of in situ SST on a global basis. The Pathfinder SST fields (Kilpatrick et al., 2001), being a satellite-based measurement, would be suitable for AIRS validation, but since the coefficients used in the atmospheric correction algorithms are derived retrospectively, these fields will not meet the near-real time requirement for the initial AIRS radiometric validation. The SSTs derived from the MODIS on *Aqua* would also be a valuable validation source, but for the fact that they too will be being undergoing initial validation at the same time as AIRS. Over the longer period of the *Aqua* mission, comparisons between data from the two sensors will be a useful approach to detect possible calibration drifts or other long period sources of uncertainty.

Buoy data are none-the-less relatively sparsely distributed and the number of match-ups with AIRS radiances will be low especially during the early phase of the mission. During the first three months of instrument operation, spaceship maneuvers combined with onboard engineering calibration exercises will limit the time spent viewing Earth scene. To obtain quick assessments of the AIRS radiances, comparisons will be made with mapped SST products. Interpolated SST fields derived from blending of in situ and satellite data allow frequent sampling of SST on a uniform grid. The NOAA operational global sea surface temperature analysis described by Reynolds and Smith (1994) and the NCEP SST-RTG have a similar origin (Reynolds and Smith, 1994). The SST analyses are produced on a uniform grid through optimum interpolation of in situ (ship and buoy) and satellite Advanced very High Resolution Radiometer (AVHRR) SST retrievals. Satellite biases relative to the in situ data are corrected using Poisson's equation prior to interpolation. The Reynold's Product is generated on a weekly basis with  $1^\circ$  spatial resolution, while

the current SST-RTG is produced daily on a  $0.5^\circ$  grid. Each use the analysis from the preceding day or week as the first guess field.

The bulk SSTs measured on buoys are decoupled from the skin SST, the source of the AIRS signal in the transparent window channels, by the thermal skin effect, and, in cases of high insolation and low wind speed, by the diurnal thermocline in the uppermost few meters of the oceanic water column (e.g. Donlon et al., 2002). There are very few instruments capable of measuring routinely the skin SST to the required accuracy, and one type of these, the Marine-Atmospheric Emitted Radiance Interferometer (M-AERI; Minnett et al., 2001), will be used in the AIRS validation. The M-AERI is a robust, accurate, self-calibrating, sea-going Fourier-transform infrared spectroradiometer that is mounted on ship to measure the emission spectra from the sea surface and atmosphere. Spectral measurements are made in the range from  $550$  to  $3000$   $\text{cm}^{-1}$  ( $\sim 3$  to  $\sim 18$   $\mu\text{m}$  wavelength), and are calibrated using two internal, NIST-traceable blackbody cavities. The environmental variables derived from the spectra include the surface skin temperature of the ocean with an absolute uncertainty of  $<0.1\text{K}$ .

The statistics of the validation data products relative to co-located drifting buoy data are shown in Table 2. The statistics of some additional products are also shown including some comparisons with M-AERI data. The TRMM Microwave Imager (TMI) SST is produced between  $\pm 40^\circ$  latitude at  $0.25$  degree resolution using a combination of three channels (Wentz, 1997). The Moderate Resolution Imaging Spectroradiometer (MODIS) is a wide-swath ( $2330\text{km}$ ), 36-channel visible and infrared radiometer on the EOS (Earth Observing System) *Terra* and *Aqua* satellites, with good SST capabilities (Esaias et al, 1998 ; Minnett et al, 2002). The accuracies of AVHRR SST Pathfinder product relative to buoy data are based on a multi-year data record (Kilpatrick et al., 2001). The statistics of these products are similar. For initial evaluation of calibrated AIRS radiances in the window channels, we have opted to use Reynolds and the daily SST-RTG product, although other products would work equally as well.

As described earlier, biases in satellite data relative to in situ observations are corrected in the surface analysis products. AIRS will measure thermal emission originating from the surface skin temperature, which can differ from bulk due to microphysical effects at the surface. These effects

Table 2. Matchup statistics between mapped SST products and drifting buoys for December 15, 2000. AIRS data sets were filtered to remove temperature differences in excess of  $\pm 3K$ . 240 granules of AIRS simulated radiances were processed for buoy comparisons. One granule was processed for M-AERI.

| Daily Matchups                             |  |
|--|--|
| SST-RTG minus buoy                         | $0.04 \pm 0.66$ (N=236)                          |
| Reynolds minus buoy                        | $0.08 \pm 0.63$ (N=294)                          |
| TMI minus buoy                             | $0.23 \pm 0.62$ (N=424)                          |
| Simulated AIRS radiances*                  |  |
| AIRS (2616 $\text{cm}^{-1}$ ) minus buoy   | Global (Day and night)<br>$0.25 \pm 1.30$ (N=74) |
| AIRS ( 938 $\text{cm}^{-1}$ ) minus buoy   | $0.09 \pm 1.44$ (N=74)                           |
| Simulated AIRS radiances*                  |  |
| AIRS (2616 $\text{cm}^{-1}$ ) minus M-AERI | Regional (Night)<br>$-0.02 \pm 0.35$ (N=40)      |
| AIRS ( 938 $\text{cm}^{-1}$ ) minus M-AERI | $-0.07 \pm 0.43$ (N=40)                          |
| Multi-year Matchups                        |  |
| AVHRR minus buoy <sup>◇</sup>              | $0.02 + 0.53$ (N>12000)                          |
| AVHRR minus M-AERI <sup>§</sup>            | $0.07 + 0.31$ (N=219)                            |
| MODIS minus M-AERI <sup>†</sup>            | $0.20 + 0.26$ (N=242)                            |

\* Relatively clear-sky conditions.

◇ Taken from Kilpatrick et al. (2001).

§ Taken from Kearns et al. (2000).

† Taken from Minnett et al. (2002).

have been measured by numerous experiments, recently described by Kearns et al. (2000) and Donlon et al. (2002). Kearns et al. compared buoy and ship intake data with radiometric sea surface measurements obtained by MAER-Is. Their observations show differences between bulk and skin temperatures under well mixed surface conditions at night to be nominally about 0.2 K, in good agreement with past observations and models of thermal skin effects (Donlon et al., 2002). The statistical uncertainty in this bias sets the lower limit of comparative analyses between SST analysis products and AIRS window radiance measurements.

The statistical accuracy that can be achieved from comparisons with shipboard radiometric measurements is limited mainly by instrument calibration. Minnett (2002) describes a careful comparison of M-AERI and MODIS data and demonstrates the high accuracies that can be achieved using shipboard measurements. Comparisons have been made between the SSTs derived from the Terra MODIS and M-AERI data from cruises in a wide range of climatic conditions.

Results from four cruises, in the Mediterranean Sea (R/V Urania, April 2000), the Pacific Ocean (USCGC Polar Sea, March – April 2001; and NOAA S Ronald H. Brown, March – April 2001), and the Eastern Caribbean (Explorer of the Seas (Prager et al., 2002), April 2001) show a mean error (MODIS – M-AERI) of 0.20K with a standard deviation of 0.26K (N=242). These are initial results that will be revised as comparisons with more cruises are analyzed.

The use of the M-AERIs to validate satellite-derived SST produce estimates of uncertainties that are significantly lower than those determined using in situ, bulk SSTs from buoys. This is because the contribution to the error budget of the variable temperature structure in the top few meters of the water column, attributed to uncertainties in the satellite-derived SST, is removed in the skin SST comparison. However, the need to provide rapid assessment of the accuracy of the AIRS in the first few months of the mission prevent reliance on the radiometric skin SSTs, and acceptance of the larger number of buoy data, even at reduced accuracy.

#### 4. VALIDATION IN THE FIRST THREE MONTHS

The basic Earth Observing System data distribution packet is a granule. For AIRS, a granule is composed of 6 minutes of AIRS data, which is equivalent to 135 cross track scans with 90 fields-of-view sweeping look angles between  $-49^\circ$  to  $+49^\circ$  and mapping an area approximately  $2000 \text{ km}^2$ . The size of the granule and the sampling resolution of AIRS are compatible with mapped SST products. The histograms of Figure 3 were obtained from differencing Reynold's SST weekly climatology and simulated AIRS radiances at  $2616 \text{ cm}^{-1}$ , *i.e.*  $3.823 \text{ }\mu\text{m}$  wavelength (a 'super' transparent short wave channel), over tropical ocean limited to the nighttime satellite pass, to avoid daytime affects of short wave scattering of solar radiation. Four different granules for simulation dates December 15, 2000, and September 13, 1998, (Fishbein et al., 2002) are represented in this figure under cloud conditions ranging from about 60 to 90% cloud cover. The AIRS radiances were "adjusted" to the surface to account for effects of atmospheric

absorption and non-unity of surface emission using an equation in simple form, with adjustment terms derived from radiative transfer calculations (Strow et al., 2002):

$$T_{\text{surf}}(\nu) = BT_{\text{TOA}}(\nu) + 0.3 \text{ K}/(\sec(\theta)) + 0.72\text{K},$$

where  $\theta$  is viewing angle.

The histogram of temperature differences for Granule 84 was obtained in the clearest region of the four cases. The histogram peaks near 1 K. For less transparent conditions, the peak broadens and shifts from zero as seen by the distribution for Granule 99. This suggests that even if the cloud distribution is poorly known per field of view, the accuracy of the instrument response can be assessed in the window regions, albeit crudely. The histogram of Figure 4 suggests that the technique works best for short wave channels.

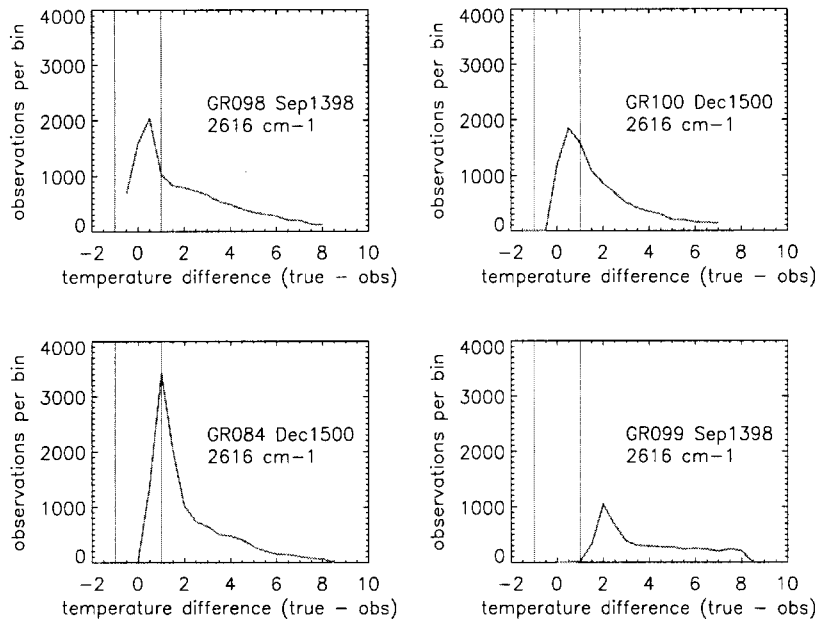


Figure 3. Histograms of the difference between SST and AIRS simulated radiances for four different granules for a window channel located at  $2616 \text{ cm}^{-1}$ . The cloud contribution to the simulated radiance is larger for Granule 99 (lower right) than the other cases. The granules were selected from tropical regions.

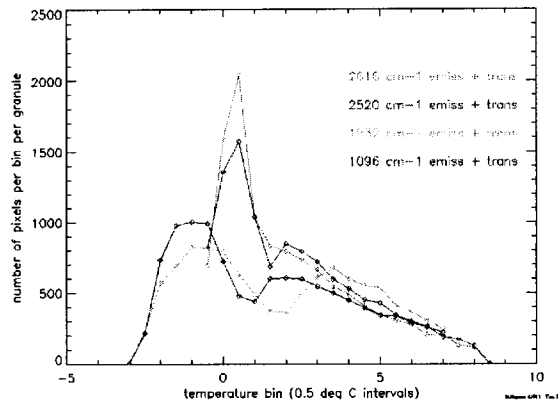


Figure 4. As in Figure 3, but showing distribution for four different window channels in a granule that is relatively cloud-free.

The statistics of the granule comparisons can be improved by applying simple threshold and cloud homogeneity tests. A spatial coherence technique (Coakley and Bretherton, 1982) using the 4  $\mu\text{m}$  window channel for identification of clear fields-of-view was tested using 34 granules located over the Pacific Ocean during night passes for the simulation of December 15, 2000. The test assumes that the surface temperature forecast over ocean is unbiased. The results, derived from 408,510 AIRS footprints, are shown in Figure 5 as two histograms, one with and without spatial coherence filtering. The upper histogram shows the distribution of the forecast SST minus AIRS simulated brightness temperatures at 2616  $\text{cm}^{-1}$  without spatial coherence filtering. The AIRS brightness temperatures have been adjusted to the surface for effects of atmospheric transmission and non-unity in surface emission, as described earlier. The mode of the histogram is less than 0.05 K. The distribution of the data suggest that, if no instrument anomalies are present, the granule comparisons should enable an assessment of the absolute accuracy of the AIRS radiances to better than an equivalent temperature uncertainty of 1 K.

## 5. VALIDATION IN THE FIRST SIX MONTHS

Sea surface temperature (SST) analysis products provide a statistical advantage over point measurements, since products are generated daily (or longer) at uniform grid points globally. However, errors related to extrapolated data in time and space can be difficult to resolve, especially in

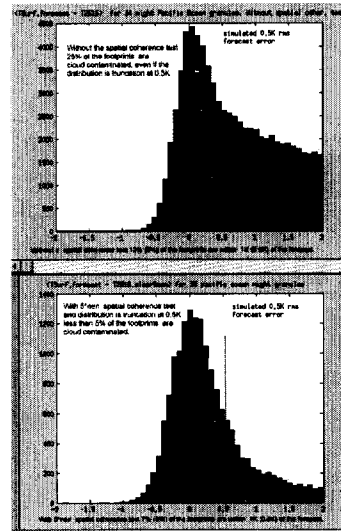


Figure 5. Histograms showing the improved statistical distribution of AIRS brightness temperature at 2616  $\text{cm}^{-1}$  minus SST surface product, with and without spatial coherence cloud filtering. The white line shows the expected distribution if no clouds are present.

real world conditions where clouds are ubiquitous. Hence, match-ups between surface marine point observations and the AIRS radiances will be initiated after launch and continued until enough 'clear sky' match-ups are available to allow meaningful statistical comparisons for each of the window regions shown in Table 1. Based on the number of drifting buoys in operation, this should require at least one month of observations. The data points in Figure 6 show the global distribution of drifting buoys for December 15, 2000. There are typically over 700 buoys operating, with the largest percentage located in the low latitudes. The buoys report every third day, so assuming 10-20% report

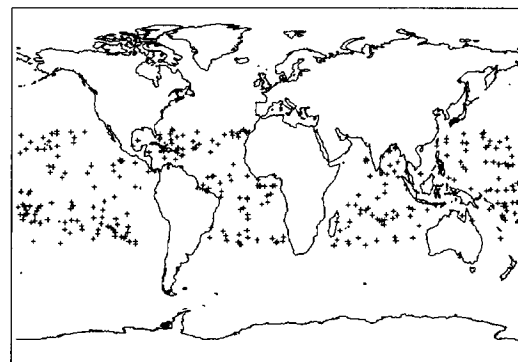


Figure 6. Distribution of drifters in low latitudes for December 15, 2000.

under cloud-free conditions, a robust data set can be acquired in 30 days.

Drifter match-ups were carried out for the AIRS Golden Day simulation of December 15, 2000, to determine if useful information could be extracted from a more limited data set. Drifter data were matched within  $\pm 50$  km and two hours of the AIRS simulated observations in the two window regions at  $2616\text{ cm}^{-1}$  and  $938\text{ cm}^{-1}$  (Table 1). Since the AIRS simulated data have no instrumental effects except noise, these channels are representative of near-by channels. The brightness temperatures for the two wavelength regions were adjusted to the surface as described earlier. Clouds were identified using a split window cloud detection routine that is based on the difference between brightness temperatures at  $911\text{ cm}^{-1}$  and  $1251\text{ cm}^{-1}$ .

Because the atmospheric opacity is low in the short wave window channels in clear sky conditions, comparisons of co-located drifting buoy observations and AIRS radiances should be similar. This is demonstrated by the data of Figure 7 for window channel  $2616\text{ cm}^{-1}$ . The analysis was derived from matchups where each point represents one cloud-free AIRS field-of-view per drifting buoy measurement. The AIRS data are corrected for scan angle effects and adjusted for non-blackness in surface emission, which together represent less than 1 K of temperature correction. The comparison includes both day and night observations. No corrections were made for solar reflectivity, so the combined contributions of reflected radiance and unresolved clouds result in large outliers. Ignoring differences exceeding  $\pm 3$  K, for 74 relatively 'clear sky' match-ups the mean and standard deviation of the data are 0.25 and 1.3 K, respectively.

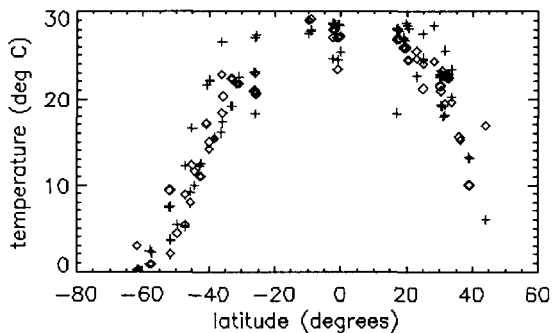


Figure 7. Zonal distribution of relatively cloud-free match-ups between drifting buoy data (black) and AIRS simulated brightness temperatures (red) at  $2616\text{ cm}^{-1}$ , adjusted to the surface. Includes day and night observations. No corrections were made for solar reflectivity.

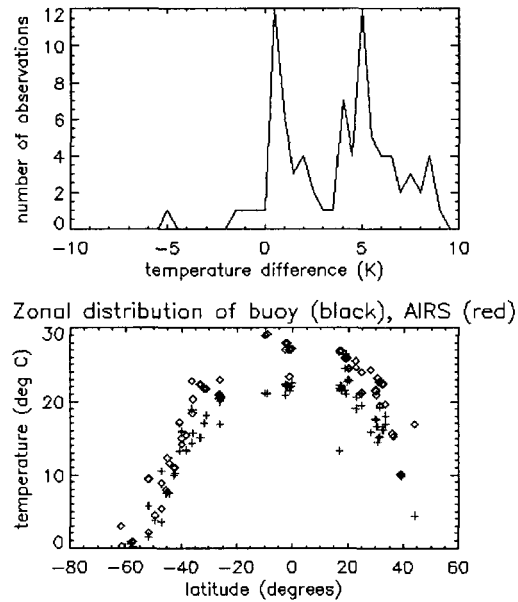


Figure 8. (a) Histogram of the differences between measured SST and AIRS simulated brightness temperatures at the top-of-the-atmosphere for a window channel located at  $942\text{ cm}^{-1}$  and (b) the distribution of data with latitude.

SST and AIRS brightness temperature equivalent to the TOA radiance at  $942\text{ cm}^{-1}$  are compared in Figure 8. Analyses in this spectral region are more complex because of water vapor continuum effects.

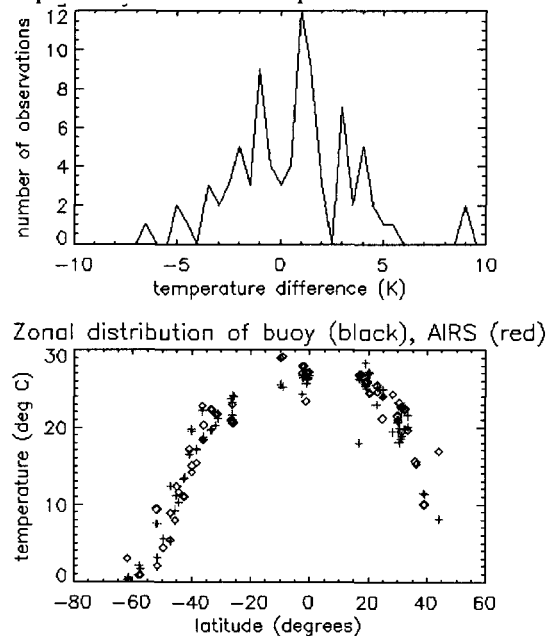


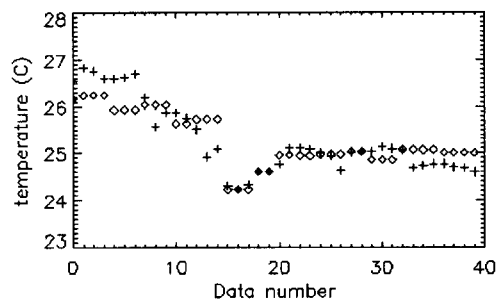
Figure 9. Same as Figure 8, but for AIRS data adjusted to the surface.

The data show a bimodal distribution with a peak in the difference histogram near 5 K. However, when corrected for effects of atmospheric transmission and non-unity in surface emission, the data redistribute with near zero bias as shown in Figure 9. The corrections resemble those for the short-wave regions, except include a moisture correction that increases as a function of different temperature regime. Ignoring differences exceeding  $\pm 3$  K, for 74 relatively ‘clear sky’ match-ups the mean and standard deviation of the data are 0.09 K and 1.44 K, respectively.

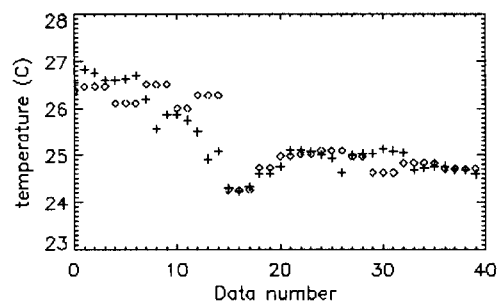
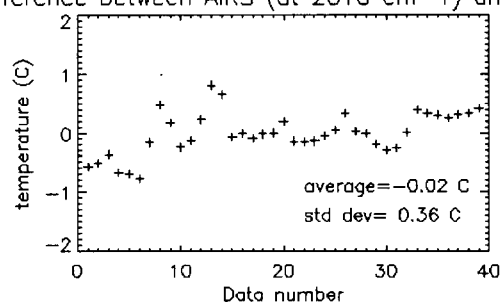
Ocean surface heating in low wind conditions was not simulated for the Golden Day data set. For the real observations, it may be necessary to eliminate data comparisons affected by surface heating, or correct the drifter measurements to the surface using a model as, for example, done by Merchant and Harris (1999). Skin versus bulk temperature differences are not considered problematic for ship-based radiometric measurements. The data of Figure 10 show differences between M-AERI observations acquired on the cruise ship *Explorer of the Seas* (Prager et al., 2002) in the Caribbean on December 15, 2000, and the AIRS brightness temperatures adjusted to the surface as previously described. The data were matched to within  $\pm 15$  km. As before, a split window cloud detection test was applied. The statistics of the match-ups are approximately the same for the window channels located at  $2616\text{ cm}^{-1}$  and at  $938\text{ cm}^{-1}$  ( $3.823\mu\text{m}$  and  $10.661\mu\text{m}$ ), and the biases are well within the desired accuracy criteria for absolute radiance validation. The statistics of the M-AERI and drifting buoy observations for the Golden Day (December 15, 2000) simulation are provided in Table 2. The drifter comparisons are noisier, but this could be related to more relaxed bounds on the spatial criteria for co-location, cloud contamination and, in the case of the short wave channel, reflected solar radiance.

## 6. SUMMARY

We have described a statistical method for early validation of the AIRS radiances over ocean that begins with night only comparisons of short wave channels to mapped SST products, and proceeds to more accurate comparisons in seventeen short and longwave window channels using ship and drifter data. The technique has been applied to surface marine data for December 15, 2000, and to simulated AIRS radiances. The simulated top-of-atmosphere radiances were adjusted to the surface



Difference between AIRS (at  $2616\text{ cm}^{-1}$ ) and MAERI



Difference between AIRS (at  $938\text{ cm}^{-1}$ ) and MAERI

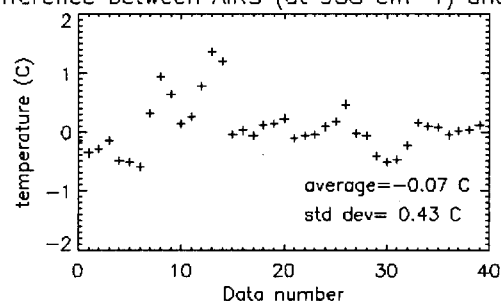


Figure 10. (a) and (c) AIRS brightness temperatures (adjusted to surface) compared with M-AERI SST, (b) and (e) AIRS brightness temperatures minus M-AERI SST for December 15, 2000, in the Caribbean.

to account for the spectral dependence of atmospheric continuum absorption and surface emission, and then differenced from SST observations. For mapped SST data over a region the size of an AIRS data granule (about  $2000\text{ km}^2$ ),

this methodology was found to work reasonably well in the short wave channels at night, yielding modes in the difference histograms which peak near 0.5 K for regions of ocean with moderate cloud cover.

A similar demonstration was carried out with ship and buoy point comparisons. The AIRS spectrometer measurement precisions, coupled with other uncertainties in the validation method excluding undetected cloud, have root-sum-square values of 0.19 K at 2616 cm<sup>-1</sup> and 0.32 K at 938 cm<sup>-1</sup>. These values are consistent with comparisons of ship-based M-AERI observations to AIRS simulated brightness temperatures, which show dispersions of just 0.4 K and bias that is negligible. If uncertainty for undetected cloud is also included, the root-sum-square values increase to about 0.6 K.

While it was not anticipated that useful statistics could be obtained from global match-ups of drifting buoy data for a single comparison day, the statistics show biases that are close to the desired calibration accuracy. The goal of the validation will be to accumulate AIRS matchups with drifting buoy data over a period of several weeks, hence reducing the overall dispersion of the data.

And finally, ocean surface heating effects are not addressed here although this is a potential source of bias error. The validation comparisons may require models to adjust bulk temperature to the surface, or alternatively, techniques that identify and exclude observations the accuracies of which have been compromised by anomalous heating.

#### REFERENCES

- Aumann, H. H., M. Chahine, K. Gautier, M. Goldberg, E. Kalnay, L. McMillin, H. Revercomb, P. Rosenkranz, W. Smith, D. Staelin and L. Strow. "AIRS/AMSU/HSB on the Aqua Mission. Design, Science Objectives and Data Products." Submitted to TGRS-IEEE EOS *Aqua* Special Issue.
- Coakley, J. A., Jr., and F. P. Bretherton (1982). "Cloud cover from high resolution scanner data: Detecting and allowing for partially filled fields of view." *J. Geophys. Res.* **87**: 4917-4932.
- Donlon, C. J., P. J. Minnett, C. Gentemann, T. J. Nightingale, I. J. Barton, B. Ward and J. Murray (2002). "Towards improved validation of satellite sea surface skin temperature measurements for climate research." *J. Climate* **15**: 353-369.
- Emery, W. J., D. J. Baldwin, P. Schlüssel and R. W. Reynolds (2001). "Accuracy of in situ sea surface temperatures used to calibrate infrared satellite measurements." *Journal of Geophysical Research* **106**(C2): 2387-2405.
- Esaias, W.E., M.R. Abbott, I. Barton, O.B. Brown, J.W. Campbell, K.L. Carder, D.K. Clark, R.H. Evans, F.E. Hoge, H.R. Gordon, W.M. Balch, R. Letelier, and P.J. Minnett. (1998) "An Overview of MODIS Capabilities for Ocean Science Observations.," *IEEE Transactions on Geoscience and Remote Sensing*, vol. 36, p. 1250-1265.
- Fishbein E., D. Gregorich D., M. Gunson M., M. Hofstadter, S.L. Lee, P. W. Rosenkranz, L. Strow, "Formulation and Validation of Simulated Data for the Atmospheric Infrared Sounder (AIRS)", submitted to TGRS-IEEE EOS *Aqua* Special Issue.
- Harris, A. R. and M. A. Saunders (1996). "Global validation of the along-track scanning radiometer against drifting buoys." *J. Geophys. Res.* **101**(C5): 12,127-12,140.
- Kilpatrick, K. A., G. P. Podesta, and R. Evans (2001). "Overview of the NOAA/NASA advanced very high resolution radiometer Pathfinder algorithm for sea surface temperature and associated matchup database." *J. Geophys. Res.* **106**(C5): 9179-9197.
- Merchant, C. J. and A. R. Harris, (1999). "Toward the elimination of bias in satellite retrievals of sea surface temperature 2. Comparison with in situ measurements." *J. Geophys. Res.* **104**(C10): 23,579-23,586.
- Minnett, P.J., R.H. Evans, E.J. Kearns and O.B. Brown. Sea-surface temperature measured by the Moderate Resolution Imaging Spectroradiometer (MODIS). *Proceedings of the IEEE International Geosciences and Remote Sensing Symposium*. Toronto, Canada June 24-28, 2002.
- Pagano, T. S., H. H. Aumann, D.E. Hagan, and K. Overoye. (2001) "Prelaunch and In-flight Radiometric Calibration of the Atmospheric Infrared Sounder (AIRS)", submitted to TGRS-IEEE EOS *Aqua* Special Issue.
- Prager, E., P. J. Minnett, B. Albrecht, H. Maring, P. Ortner, D. Wilson, S. Cummings, D. Palmer and E. Williams (2002). "Explorer of the Seas: A Revolution in Marine Research and Education." *EOS, Trans. Am. Geophys. Union*. In preparation.

- Reynolds, Richard and T. M. Smith (1994).  
“Improved global sea surface temperature  
analyses using optimum interpolation.” J.  
Climate 7: 929-948.
- Strow, L., S. Hannon, M. Weiler, S. Gaiser and H.  
Aumann. “AIRS Prelaunch Spectral  
Characterization and In-orbit Calibration.”  
Submitted to TGRS-IEEE EOS *Aqua*  
Special Issue.
- Strow, L., S. Hannon, S. Desouza-Machado, D.  
Tobin, H. Motteler. “AIRS Radiative  
Transfer Algorithm Development and  
Validation.” Submitted to TGRS-IEEE  
EOS *Aqua* Special Issue.
- Wentz, F. J., C. Gentemann, D. Smith and D.  
Chelton (2000), “Satellite measurements  
of sea surface temperature through  
clouds.” Science 288: 847-850.